PNAS

www.pnas.org

Supplementary Information for

The structural role of bacterial eDNA in the formation of biofilm streamers.

Eleonora Secchi[1], Giovanni Savorana[1], Alessandra Vitale[2], Leo Eberl[2], Roman Stocker[1] and Roberto Rusconi[3,4]

* Eleonora Secchi.

Email: esecchi@ethz.ch

This PDF file includes:

> Supplementary text
> Figures S1 to S16
> Legends for Movies S1 and S2
> SI References

Other supplementary materials for this manuscript include the following:

> Movies S1 and S2

Supplementary Information Text

Statistics and derivations

All image analysis was performed in Fiji-Image J (1). All images of streamers are examples from experiments that were repeated three times with consistent results.

The average fluorescence intensity of the streamers in each channel was calculated on the red fluorescence signal as

$$\bar{I}_{str} = \langle \Sigma (I_{px} - I_{th}) \rangle_{channel},$$

where I_{px} is the intensity of the pixels, and I_{th} is a threshold calculated as 1.2 times the average intensity of the background, I_{back}, measured in the region of the channel on the side of the streamer. The sum was performed on a 550 µm × 100 µm area located downstream of each pillar (white dotted line in Fig. S2) and averaged over the six pillars contained in each channel. During each experiment, multiple channels with the same conditions were present and the average fluorescent intensity of the streamers $\langle \bar{I}_{str} \rangle$ reported in the figures was obtained as an average over channels under the same experimental conditions. The same procedure was used to calculate the average fluorescence intensity on the pillar surface, $\langle \bar{I}_{pill} \rangle$. In this case, the sum was performed on an area of dimensions 55 µm × 100 µm located around the pillar (yellow dotted line in Fig. S2).

The diameter and length of streamers were measured on the fluorescence images of the red signal. The streamer was identified as the region of the image where the intensity of the pixels, I_{px}, exceeded the threshold, I_{th}. The diameter of the streamer was defined as the width of the filament in the direction perpendicular to the flow. The diameter of the streamer in the region close to the pillar, d_{150}, was averaged over a distance of 150 µm from the pillar. The diameter of the streamer in the region downstream from the pillar, d_{400}, was taken as the average of the width from 400 µm to 1000 µm from the pillar. To measure the length of the streamer, L, images were stitched together using the Stitching Plugin in Fiji-Image J.

The coverage of the channel's bottom surface, C_{surf}, was defined as the percentage of the surface covered by cells and was calculated on phase-contrast images of the surface of the channel. One region with dimensions 670 µm × 670 µm, located 3 mm upstream from a pillar and free from the presence of the streamer, was considered for each channel. Bacterial cells appeared as darker spots and their area was estimated as the number of pixels with an intensity lower than 0.8 × $I_{surface, ph}$, where $I_{surface, ph}$ is the average gray intensity of the bacteria-free surface acquired in phase-contrast. In Fig. 5, we report the average red fluorescence intensity of the surface, $\langle \bar{I}_{surface,red} \rangle$, which was defined as the average red fluorescence intensity (corresponding to the PI signal) in the region with dimensions 670 µm × 670 µm used to calculate the surface coverage.

Values of d_{150}, d_{400}, L, $\langle \bar{I}_{str} \rangle$, $\langle \bar{I}_{pill} \rangle$ and C_{surf} reported in Fig. 2 were measured for each experiment and the values were averaged over two channels with identical experimental conditions. The error bars represent the standards deviations of the mean. The *Pel intensity* shown in the inset of Fig. 2*F* was calculated using the same definition of $\langle \bar{I}_{str} \rangle$ on single images of streamers formed after 20 h of continuous flow and stained first with WF for 30 min and then with PI for 30 min (sample images shown as Fig. S1). In this case, each value is obtained as an average over six pillars and experiments were repeated twice.

$\langle \bar{I}_{str} \rangle$, $\langle \bar{I}_{pill} \rangle$ and C_{surf} reported in Fig. S6*I-K* were measured during the same experiment and the values are averaged over two channels. The same applies to Fig. S6*P-R*. In Fig. 4, the Reduction reported in panels *D-F* is defined as

$$\text{Reduction \%} = \frac{\langle x(24) \rangle_{control} - \langle x(24) \rangle_{DNase\,I}}{\langle x(24) \rangle_{control}} \times 100,$$

where $x(24)$ represents the quantity reported in the main panel ($\langle \bar{I}_{str} \rangle$, $\langle \bar{I}_{pill} \rangle$ and C_{surf}) and measured after 24 h. We refer to control as the channel in which no DNase I treatment was performed.

Reduction reported in Fig 4 panels *J-L* is defined as

$$\text{Reduction \%} = \frac{\langle x\,(21) \rangle - \langle x\,(24) \rangle}{\langle x\,(21) \rangle} \times 100,$$

where *x(21)* represents the quantity reported in the main panel ($\langle \bar{I}_{str} \rangle$, $\langle \bar{I}_{pill} \rangle$ and C_{surf}) and measured after 21 h of flow of Tryptone broth (before DNase I treatment) and *x(24)* the same quantity measured after 3 h of DNase I treatment. In this case, a negative reduction indicates an increase of the quantity during the DNase I treatment.

$\langle \bar{I}_{str} \rangle$, $\langle \bar{I}_{pill} \rangle$ and C_{surf} reported in Fig. 5 were measured during the same experiment and the values are averaged over two channels. The single-stranded DNA concentration was measured in the effluent suspension of each channel, for the point at 15 h (corresponding to the liquid sampled in the period 14.5–15.5 h) and the point at 24 h (sampled 23.5–24.5 h).

The data reported in the Supplementary are measured during the same experiments and the values are averaged over two channels. All the experiments reported were performed at least three times and, in each experiment, a consistent trend was found.

Mechanical tests

Rheological characterization was performed on streamers grown at a flow rate Q = 0.3 ml/h (average flow velocity 2 mm/s). Δ*wspF* streamers were tested after 14-15 h from the beginning of the experiment, while *WT* and Δ*pelE* after 20-22 h. Stress tests were performed by increasing the flow rate to 0.6 ml/h (average flow velocity 4 mm/s) for 5 min (red curve, Fig. S3*A*). While at this flow rate, the deformation of a portion of the streamer in the region between 400 μm and 1 mm from the pillar was imaged in phase contrast at 1 fps. Deformation was quantified by tracking the relative displacement of cell aggregates within the filaments, using the software Blender (https://www.blender.org/) (blue curve, Fig. S3*A*). The stress step applied in each experimental replicate was quantified using finite element code (COMSOL Multiphysics). The 3D model of the streamers was built for each replicate based on the eDNA signal of epifluorescence images acquired before each stress test. The results reported in Fig. 3 were calculated as the average of five independent bacterial batches, each one prepared on a different day (Fig. S3*B*, *C*), and the values of E and η for a single batch were an average over identical experiments. The error bar is the standard deviation of the mean.

eDNA assembly in flow

According to the literature about the aggregation of DNA molecules in shear flow (2, 3), shear flow can induce and control the assembly of λ-phage DNA when $\gamma\tau > 1$, where γ is the flow shear rate and τ is the relaxation time of the molecule, which depends on the size of the DNA fragments. Under this condition, DNA molecules are stretched and deformed by flow, which exposes their ends. Thus, their intermolecular interaction probability is increased, leading to inter-chain bonding and the formation of 3D elongated structures (2).

The shear rate values in a 5 μm-thick annulus around the pillar in the midplane of the channel, where eDNA aggregation is likely to happen, are in the range 280 $s^{-1} < \gamma <$ 700 s^{-1}.

The bulk values of the relaxation time, τ, can be estimated using

$$\tau = 0.1\,\eta\,\left(\frac{M}{M_{\lambda-DNA}}\right)^{1.8} s\,\text{`},$$

where η is the viscosity of the buffer (in our case water, η = 1 cP), *M* is the molecular weight of the eDNA molecule and $M_{\lambda-DNA}$ is the molecular weight of λ-DNA ($M_{\lambda\text{-DNA}}$ = 48.5 kbp) (4).

Given the limiting values for γ, we can calculate the molecular weight M of the eDNA molecules required to satisfy the condition $\gamma\tau > 1$ as

$$0.1\,\eta\,\left(\frac{M}{M_{\lambda-\mathrm{DNA}}}\right)^{1.8} > \frac{1}{\gamma}\,.$$

For $\gamma = 280\ s^{-1}$, we obtain $M > 7.6$ kbp, while for $\gamma = 700\ s^{-1}$, $M > 4.6$ kbp. In conclusion, our flow configuration promotes the assembly of eDNA molecules with $M > 4.6$ kbp.

Since eDNA released by cell lysis is similar to chromosomal DNA (5, 6) and the genome of *P. aeruginosa* is 6.3 Mbp (7), the fragments present are likely of a size for which assembly is promoted by the flow.

Impact of pH on the morphology and mechanical properties of streamers

The formation of streamers by *P. aeruginosa* was also observed under more acidic and more alkaline conditions. The pH of the culture medium was 6.6 in our main experiments, and it could be adjusted to 5.8 or 7.8 without affecting the viability of bacteria in bulk (Methods, Fig. S4 *A* and *B*). According to previous work (8), the charge of Pel when in suspension increases at pH lower than 6.8, strengthening the interaction with eDNA, while it becomes neutrally charged at higher pH values, reducing the ionic interaction with eDNA. This potential impact of pH on streamer formation was investigated by comparing the streamers formed by PA14 *ΔpelE* and PA14 *WT* at different values of pH. Biofilm streamers formed at all three values of pH tested in both strains, confirming the robustness of the described phenomenon. The variation in pH did not affect streamer morphology or the number of cell aggregates on the filament (Fig. S4*C*). However, variation in pH altered the rheological properties of the streamers. In comparison with the rheology of the control (pH 6.6), we found opposite effects of changing pH in the wild-type strain and the Pel-deficient mutant. In the case of PA14 *WT*, both the acidic and the alkaline pH induced a twofold increase in the elastic modulus E and a 50% increase in the effective viscosity η, resulting in a stiffer filament (blue circles in Fig. S4 *D* and *E*); conversely, in the case of PA14 *ΔpelE*, both the acidic and alkaline pH induced a 50% decrease E and η (red squares in Fig. S4 *D* and *E*). These differences in the viscoelastic behavior could therefore be attributed to the presence of Pel. The stiffening at acidic pH may be ascribed to the potential strengthening of the eDNA-Pel interaction, while the changes at alkaline pH cannot be explained in light of the current literature, and require further investigation.

The matrix protein CdrA does not affect the formation or the mechanical properties of PA14 streamers

The matrix protein CdrA has been shown to make a critical contribution to robust biofilm formation in flow cells by PA14 due to its capacity to bind to Pel (9). We determined the role of CdrA by comparing the streamers formed by the wild-type strain (PA14 *WT*) and by a mutant strain lacking the ability to produce CdrA (PA14 *ΔCdrA*). The CdrA-deficient mutant produced streamers with similar morphology to the *WT* (Fig. S5 *A* and *B*). CdrA-deficient streamers were on average 2.04 mm $\pm$ 0.02 mm long after 15 h, minimally (~7%) shorter than *WT* streamers (Fig. S5*C*). CdrA-deficiency did not affect the average diameter, which was equal to $d_{150} = 11$ μm $\pm$ 1 μm in the vicinity of the pillar and $d_{400} = 4.2$ μm $\pm$ 0.4 μm in the downstream region, comparable to the values for *WT* streamers after 15 h (Fig. S5*D*). The elastic modulus of *ΔCdrA* streamers ($E = 5.6$ kPa ± 0.3 kPa) and the effective viscosity ($\eta = 16.9$ MPa s ± 7.7 MPa s) were 16% and 8% higher than in the *WT,* respectively (Fig. S5 *E* and *F*). Nevertheless, these differences are marginal compared with the values obtained with the *ΔpelE* and *ΔwspF* mutant strains. Therefore, we conclude that the protein CdrA does not seem to have a strong influence on the structural and rheological properties of PA14 biofilm streamers.

eDNA degradation prevents streamer formation by *P. aeruginosa* PAO1

The formation of biofilm streamers and the inhibition of their formation with DNase I was found to be a consistent feature across other *P. aeruginosa* strains and mutants with different polysaccharide composition of the extracellular matrix. We compared streamer formation in different mutants of the PAO1

strain, including the wild-type strain (PAO1 *WT*), which incorporates both Psl and Pel into the extracellular matrix, a mutant strain lacking the ability to produce Pel (PAO1 *ΔpelA*), a mutant strain lacking the ability to produce Psl (PAO1 *ΔpslB*), and a mutant strain lacking the ability to produce both Pel and Psl (PAO1 *ΔpelA ΔpslB*). Streamer formation was observed for all PAO1 strains. Comparison among strains revealed that Psl increases the biomass trapped in the filaments (Fig. S12 *A* and *B,* upper panels) and the surface coverage of channel's lower surface (Fig. S12 *H,* and *I*, upper panels) relative to the Psl-deficient mutants (Fig. S12 *C* and D*, J* and *K,* upper panels). Conversely, Psl-deficient strains formed thinner filaments that were similar to those formed by PA14 (Fig. S12 *C* and *D*, upper panels) and displayed comparable surface colonization (Fig. S12 *J* and *K*, upper panels). When treated with DNase I solution from the beginning of the experiment, none of the PAO1 mutant strains formed streamers for the entire duration (24 h) of the experiments (Fig. S12 *A–D,* lower panels). DNase I treatment also prevented the accumulation of eDNA on the channel's lower surface (Fig. S12*F, H–K,* lower panels), but did not hamper bacterial colonization of the surface, with the different mutant strains showing either no reduction or an increase in bacterial surface coverage C_{surf} (Fig. S12*G, H–K,* lower panels). These results confirm the primarily structural role of eDNA in the formation of biofilm streamers across *P. aeruginosa* strains.

Evaluation of the viability of the bacterial suspension over the experimental timescale

To confirm that there were no changes in the viability of the in-flowing bacterial suspension while it was held within the syringe over the experimental timescale of 16 h, we performed flow cytometry and live/dead cell staining. *P. aeruginosa* PA14 *WT* cells were prepared and loaded into a 10 mL syringe following the experimental procedure reported in the Methods. A 1 mL sample was taken at the beginning of the experiment and after 16 h. Bacteria were stained with a mixture of SYTO 9 and propidium iodide (PI), following the LIVE/DEAD BacLight Bacterial cell viability kit protocol (Sigma, Switzerland), and incubated for 15 min. Bacteria were counted using flow cytometry (Cytoflex LX, Beckmann Coulter) with flow rate 10 µL/min.

The results revealed bacterial growth during the 16 h resting period in the syringe and very little cell death (Table S1).

Table S1. Cell counts in the bacterial suspension within the syringe over the experimental timescale.

| Time (h)	Live cells (events/ µL)	Live cells (%)	Dead cells (events/ µL)	Dead cells (%)
0	77.0	93.9	5.0	6.1
16	1506.8	98.9	17.4	1.1

Supplementary Figures
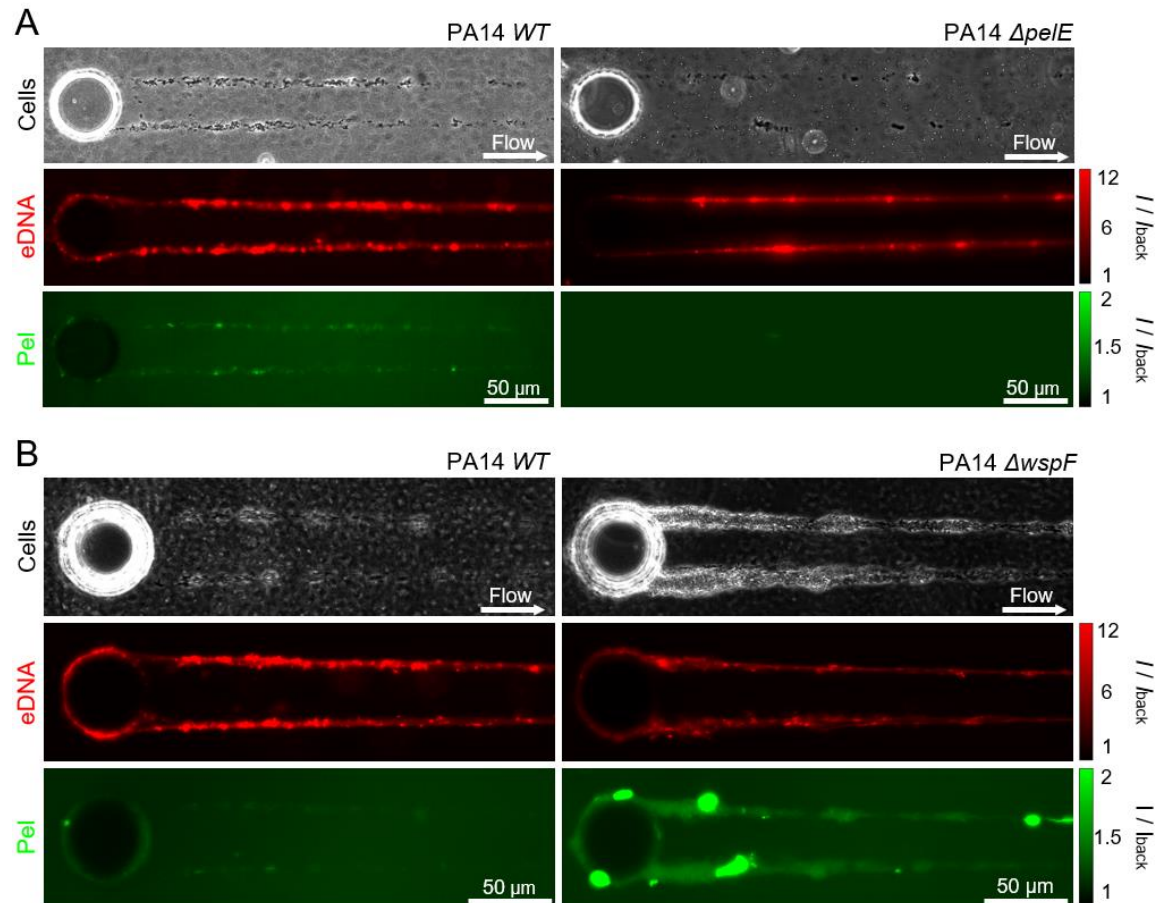
Fig. S1. Streamer formation by *P. aeruginosa* PA14. *(A-B)* Phase-contrast and fluorescence representative images of the biofilm streamers formed by *P. aeruginosa* PA14 *WT* (left) and Δ*pelE* (right) cells (*A*) and by PA14 *WT* (left) and Δ*wspF* (right) cells (*B*) attached to a 50-μm pillar after 20 h of continuous flow of a dilute bacterial suspension at U = 2 mm/s. The images were taken at channel mid-depth. Bacterial cells were imaged in phase contrast (top), eDNA was stained using red-fluorescent PI (2 μg/mL; middle), and Pel was stained using the green-fluorescent WFL (50 μg/mL; bottom). The intensity was divided by the average fluorescence intensity in the channel region not occupied by the streamer to ease the comparison of the fluorescence images.
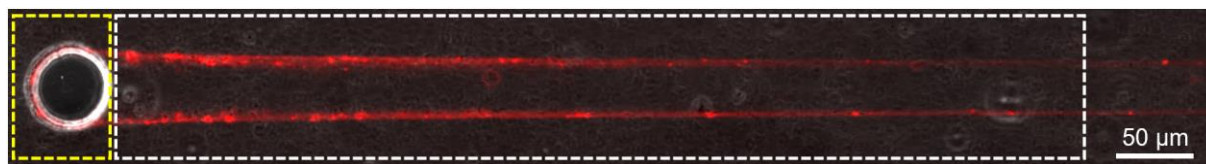
Fig. S2. Sample regions selected to quantify streamer fluorescence intensity. Average fluorescence intensity of the streamers and the biofilm around the pillar surface were measured in the regions of the image contained within the 550 μm × 100 μm dashed white box and the 55 μm × 100 μm dashed yellow box, respectively.
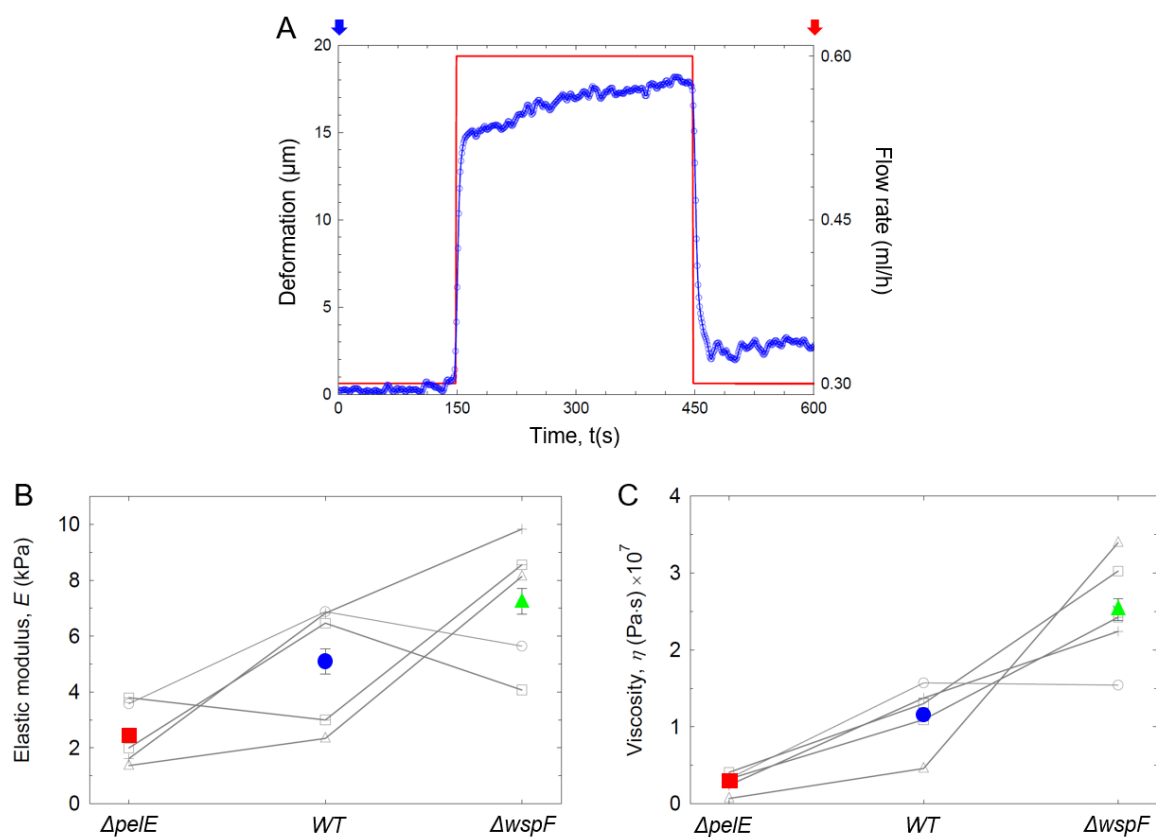
Fig. S3. Mechanical test of biofilm streamer rheological properties. (*A*) Deformation of a PA14 *WT* streamer (blue curve, left axis) undergoing the mechanical tests. The streamer was deformed by increasing the flow rate (red curve, right axis) from 0.3 ml/h (corresponding to U = 2 mm/s) to 0.6 ml/h (corresponding to U = 4 mm/s). (*B*) Elastic modulus, E, of the biofilm streamers reported in Fig. 3, obtained as the mean of five independent experimental replicates carried out on different days (gray symbols). (*C*) Viscosity, η, measured in the same experiments as Fig. 3, was obtained as the mean of five independent experimental replicates carried out on different days (gray symbols). The error bar is calculated as the standard error of the mean.
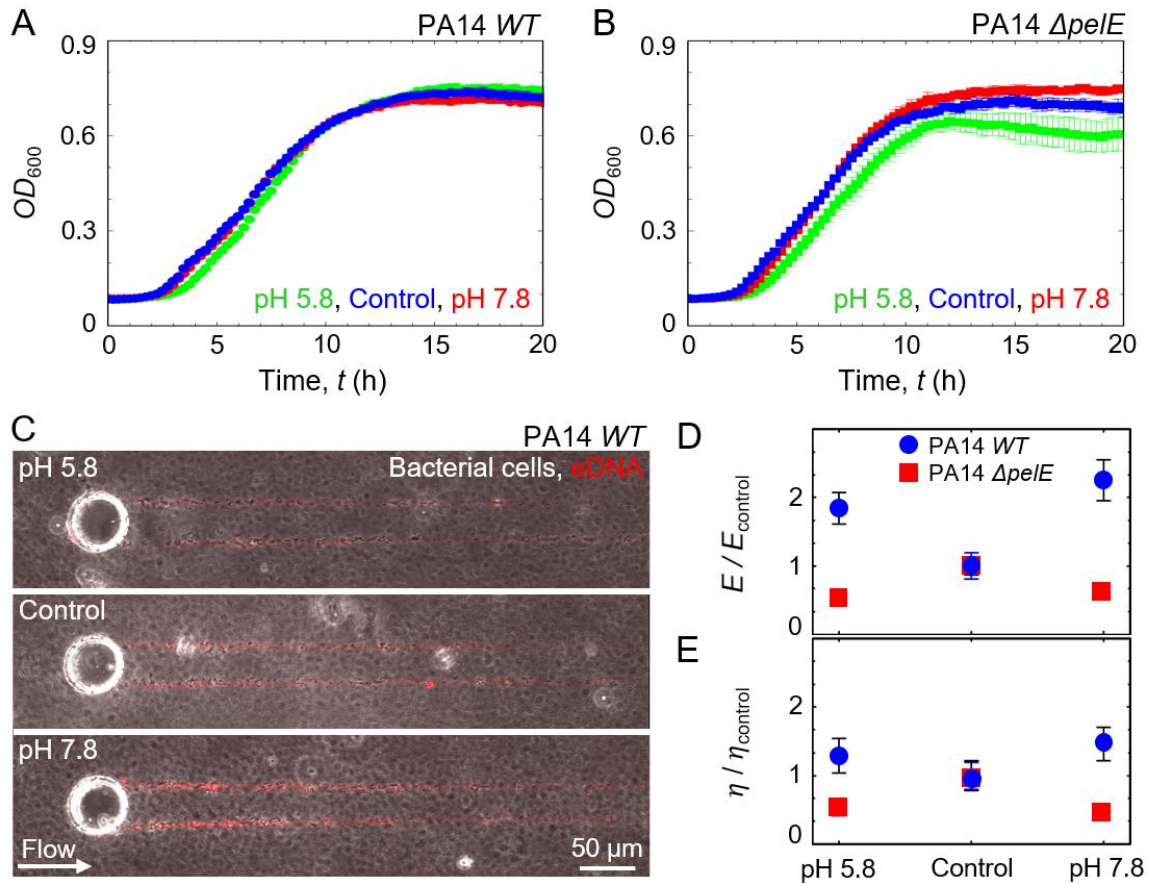
Fig. S4. Effect of pH on growth in suspension and on streamer formation in PA14 *WT* and PA14 *ΔpelE*. (*A* and *B*) Population growth (OD_{600}) of *P. aeruginosa* PA14 WT (*A*) and PA14 *ΔpelE* (*B*) cultures at 37 °C in Tryptone Broth at pH 5.8 (green), pH 6.6 (blue; control), and pH 7.8 (red). The pH of the Tryptone broth was initially 6.6 and then was adjusted to 5.8 and 7.8 by adding HCl and NaOH, respectively. Values of OD_{600} were measured using a plate reader (Sinergy HTX, BioTeck). The samples were loaded in a 96 wells plate; each curve was obtained as an average of six biological replicates. (*C*) Overlaid phase-contrast (bacterial cells) and red fluorescence (PI) representative images of biofilm streamers formed by PA14 *WT* attached to a 50-µm pillar after 15 h of continuous flow of a dilute bacterial suspension at $U = 2$ mm/s at pH 5.8 (upper panel), pH 6.6 (mid panel; control) and pH 7.8 (lower panel). The slight reduction in the red signal from the PI staining at pH 5.8 did not correspond to a difference in the phase-contrast image and was attributed to a reduced efficiency of the staining. (*D* and *E*) Elastic modulus (*D*) rescaled using the elastic modulus of the control, $E/E_{control}$, and effective viscosity (*E*) rescaled using the effective viscosity of the control, $\eta/\eta_{control}$, of biofilm streamers formed by PA14 *WT* (blue circles) and PA14 *ΔpelE* (red squares). Experimental conditions as in *C*. Points show the average of three biological replicates of each of the experiments and error bars represent the standard error of the mean.
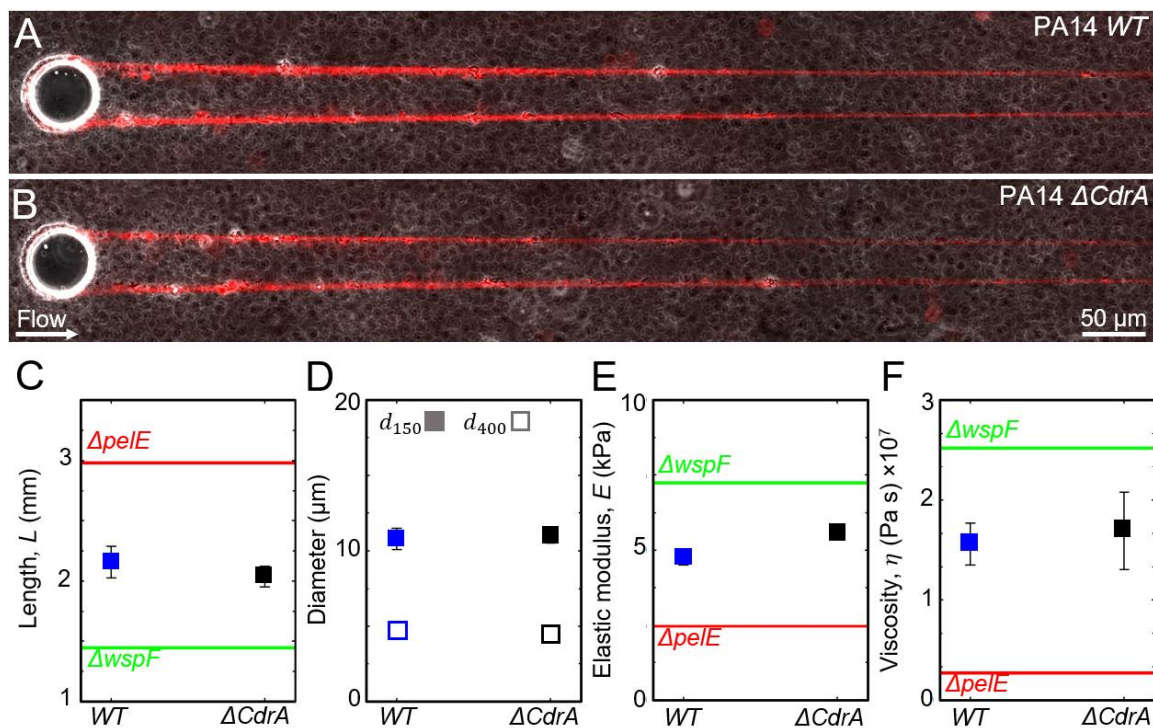
Fig. S5. The protein CdrA does not play a role in the formation or the mechanical properties of PA14 biofilm streamers. (*A* and *B*) Overlaid phase-contrast (bacterial cells) and red fluorescence (PI) representative images of biofilm streamers formed by *P. aeruginosa* PA14 wild-type, *WT* (*A*), and CdrA-deficient, *ΔCdrA* (*B*), attached to a 50-µm pillar after 15 h of flow of a dilute bacterial suspension at $U = 2$ mm/s. (*C*) Length of streamers after 15 h of flow, measured from fluorescence images for *WT* (blue) and *ΔCdrA* (black). (*D*) Diameter of streamers in the vicinity of the pillar (150 µm from the pillar, d_{150}) (filled squares) and in the downstream region (400 µm from the pillar, d_{400}) (open squares) after 15 h of continuous flow, measured from fluorescence images for the two strains. (*E* and *F*) Elastic modulus, *E* (*E*), and effective viscosity, η (*F*), of biofilm streamers formed by PA14 *WT* (blue) and *ΔCdrA* (black). In *C–F*, points show the average of three biological replicates and error bars represent the standard error of the mean. Red and green lines in *C*, *E*, and *F* indicate average values reported in Fig. 2 for *ΔpelE* (Pel-deficient) and *ΔwspF* (Pel-overproducing), respectively.
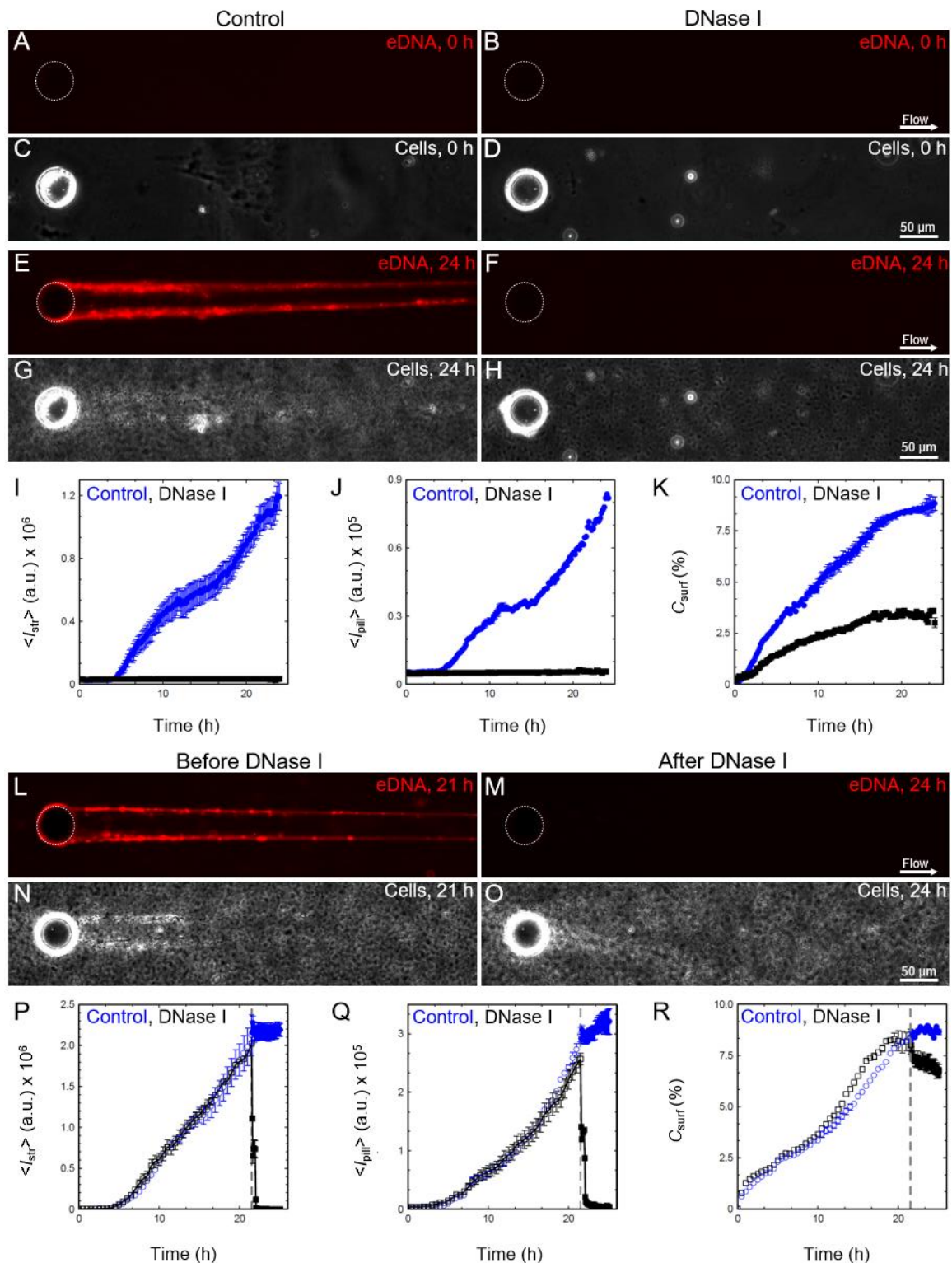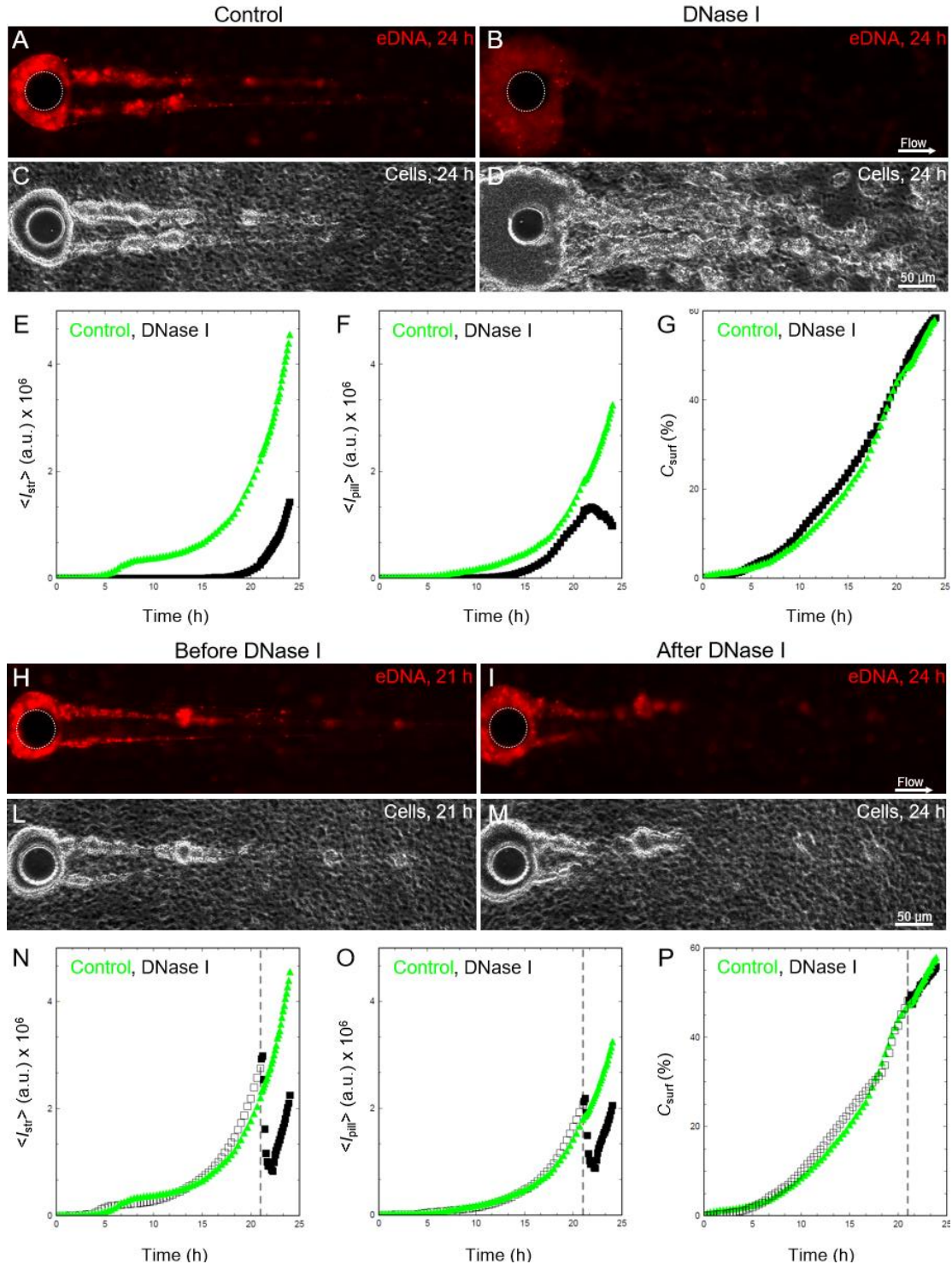
Fig. S6. DNase I prevents streamer formation by PA14 *WT* and causes degradation of established streamers. (*A–H*) Fluorescence (*A, B, E, F*) and phase-contrast (*C, D, G, H*) representative images of the biofilm streamers formed by *P. aeruginosa* PA14 *WT* cells attached to a 50-µm pillar when the flow is started (*A-D*) and after 24 h of continuous flow (*E-H*) of a dilute bacterial suspension at *U* = 2 mm/s either untreated (*A, C, E, G*) or treated with 1 mg/mL DNase I (*B, D, F, H*). (*I-K*) Fluorescence intensity of the

streamers, $\langle \bar{I}_{\mathrm{str}} \rangle$ (*I*) and of the biofilm around the pillar surface, $\langle \bar{I}_{\mathrm{pill}} \rangle$ (*J*), and surface coverage, C_{surf} (*K*) as a function of time for the same suspension in *A* with no DNase treatment (blue circles) and *B* treated with DNase (black squares). Points show the mean and standard error of the mean of two replicates. (*L-O*) Fluorescence (*L, M*) and phase-contrast (*N, O*) representative images of the biofilm streamers formed by *P. aeruginosa* PA14 *WT* cells attached to a 50-µm pillar after 21 h of continuous flow of a diluted bacterial suspension at *U* = 2 mm/s (*L, N*) and of the same streamer after 3h of treatment with 1 mg/mL DNase I (*M, O*). (*P-R*) Fluorescence intensity of the streamers, $\langle \bar{I}_{\mathrm{str}} \rangle$ (*P*) and of the biofilm around the pillar surface, $\langle \bar{I}_{\mathrm{pill}} \rangle$ (*Q*), and surface coverage, C_{surf} (*R*) as a function of time, measured during 21 h of continuous flow of a diluted bacterial suspension in Tryptone broth (open symbols) and during the following 3 h during which streamers were exposed to flow of 1 mg/mL DNase I in Phosphate Buffer Saline, PBS, (black filled squares) or just PBS (blue filled circles). Points show the mean and standard error of the mean of two replicates.
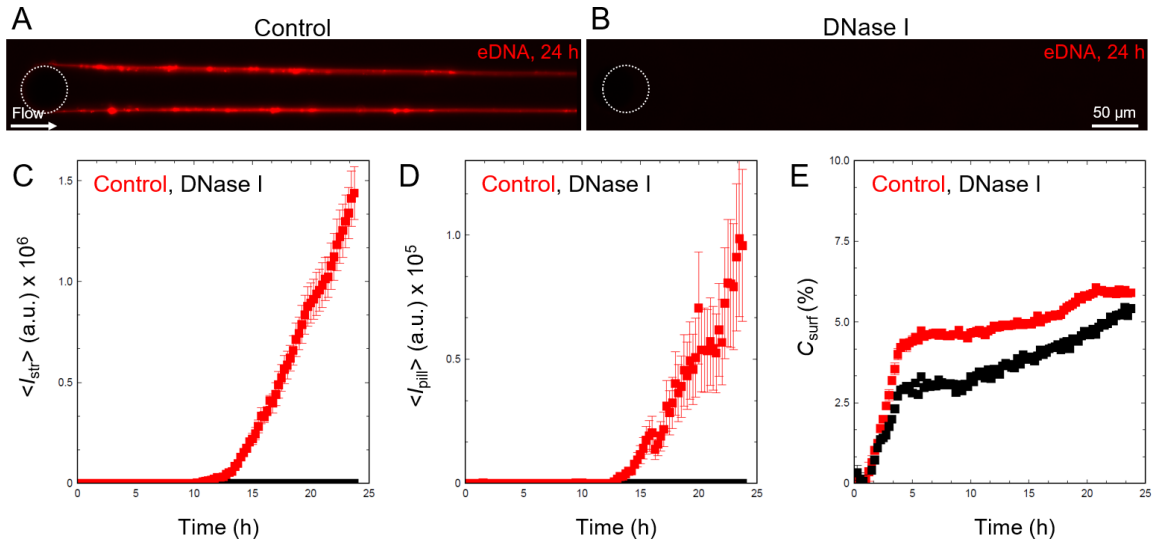
Fig. S7. DNase I prevents streamer formation by PA14 *ΔpelE*. (*A-B*) Representative fluorescent image of the biofilm streamers formed by *P. aeruginosa* PA14 *ΔpelE* cells attached to a 50-µm pillar after 24 h of continuous flow of a diluted bacterial suspension at $U = 2$ mm/s untreated (*A*) and treated with 1 mg/mL DNase I (*B*). (*C-E*) Fluorescent intensity of the streamers, $\langle \bar{I}_{str} \rangle$ (*C*) and of the biofilm around the pillar surface, $\langle \bar{I}_{pill} \rangle$ (*D*), and surface coverage, C_{surf} (*E*) as a function time for the same suspension in *A* (red squares) and *B* (black squares). Points show the mean and standard error of the mean of two replicates.

Fig. S8. DNase I prevents streamer formation by PA14 *ΔwspF* and causes degradation of established streamers. (*A-D*) Fluorescent (*A, B*) and phase contrast representative images of the biofilm streamers formed by *P. aeruginosa* PA14 *ΔwspF* cells attached to a 50-μm pillar after 24 h of continuous flow of a diluted bacterial suspension at U = 2 mm/s untreated (*A, C*) and treated (*B, D*) with 1 mg/mL DNase I. (*E-G*) Fluorescence intensity of the streamers, $\langle \bar{I}_{str} \rangle$ (*E*) and of the biofilm around the pillar surface, $\langle \bar{I}_{pill} \rangle$ (*F*), and surface coverage, C_{surf} (*G*) as a function time for the same suspension in *A* (green triangles) and *B* (black squares). (*H-M*) Fluorescence (*H, I*) and phase contrast (*L, M*) representative
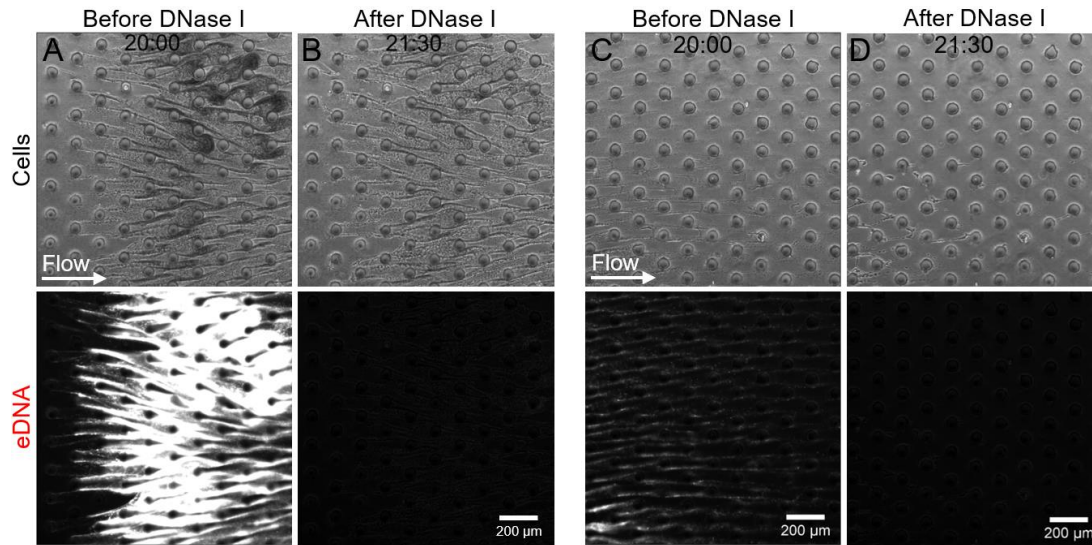
images of the biofilm streamers formed by *P. aeruginosa* PA14 *ΔwspF* cells attached to a 50-µm pillar after 21 h of continuous flow of a diluted bacterial suspension at $U = 2$ mm/s (*H, L*) and of the same streamer after 3h treatment with 1 mg/mL DNase I (*I, M*). (*N-P*) Fluorescence intensity of the streamers, $\langle \bar{I}_{str} \rangle$ (*N*) and of the biofilm around the pillar surface, $\langle \bar{I}_{pill} \rangle$ (*O*), and surface coverage, C_{surf} (*P*) as a function time measured during 21 h of continuous flow of a diluted bacterial suspension in Tryptone broth (open symbols) and during the following 3 h-treatment performed flowing 1 mg/mL DNase I in PBS (black filled squares) or just PBS (green filled triangles) for the same suspension in *H* (green triangles) and *I* (black squares).
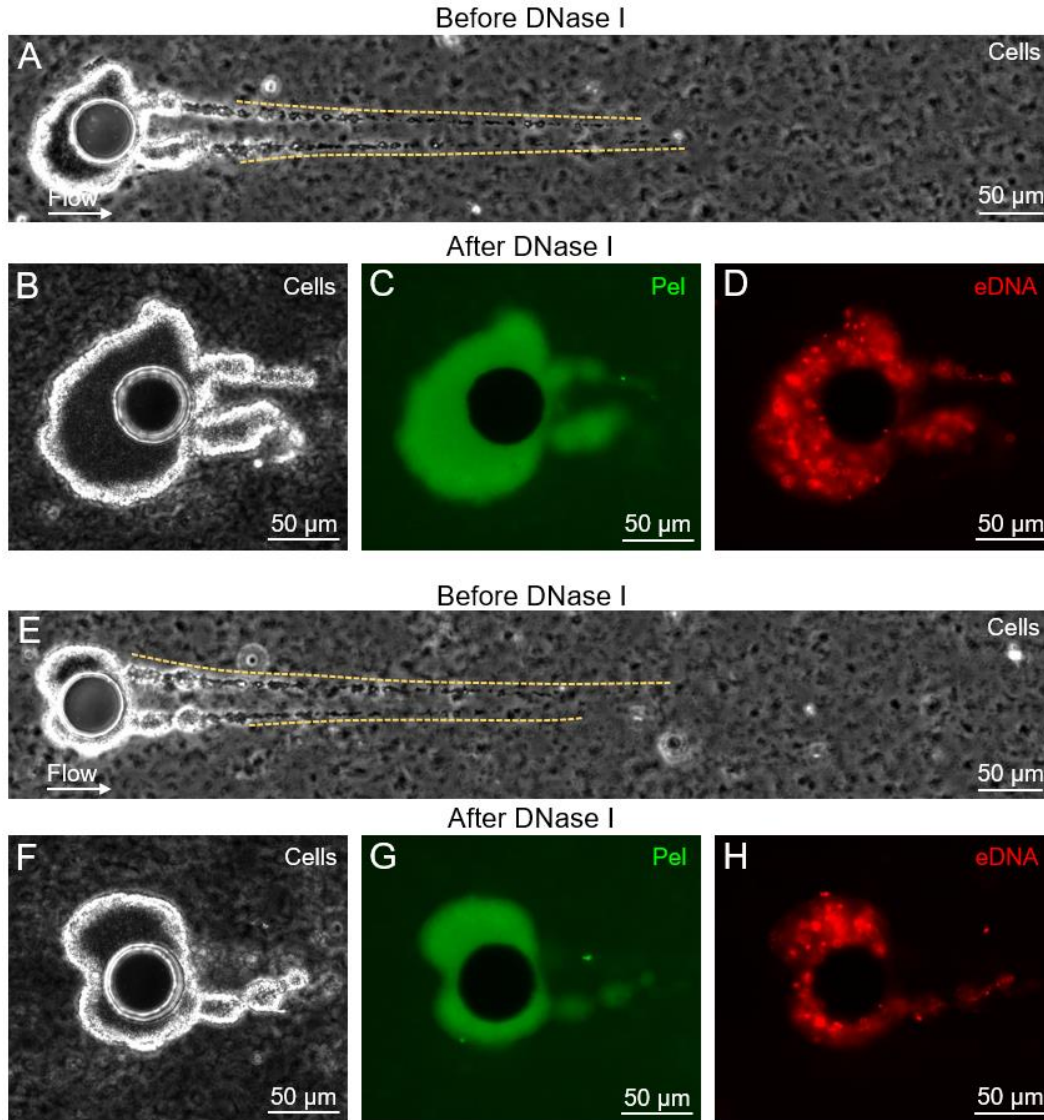
Fig. S9. Pel reduces the effectiveness of DNase I treatment on PA14 *ΔwspF* streamers. (*A-H*) Phase contrast (*A, B, E, F*) and fluorescent (*C, D, G, H*) representative images of the biofilm streamers formed by *P. aeruginosa* PA14 *ΔwspF* cells attached to a 50-μm pillar after 21 h of a continuous flow of a dilute bacterial suspension at $U = 2$ mm/s (*A, E*) and of the same streamer after 3h treatment with 1 mg/mL DNase I (*B-D, F-H*). Yellow dotted lines in *A* and *E* indicate the portions of the streamer removed during the treatments. Bacterial cells are imaged in phase contrast, eDNA is stained using red-fluorescent PI (2 μg/mL; *D, H*) and Pel is stained using the green-fluorescent WFL (50 μg/mL; *C, G*). DNase I treatment destroys the filaments, as seen by comparing the images taken before (*A, E*) and after (*B, F*) the treatment. However, the Pel-containing aggregates (*C, G*) are not affected by the treatment, as Pel appears to shield eDNA from DNase I activity (*D, H*).
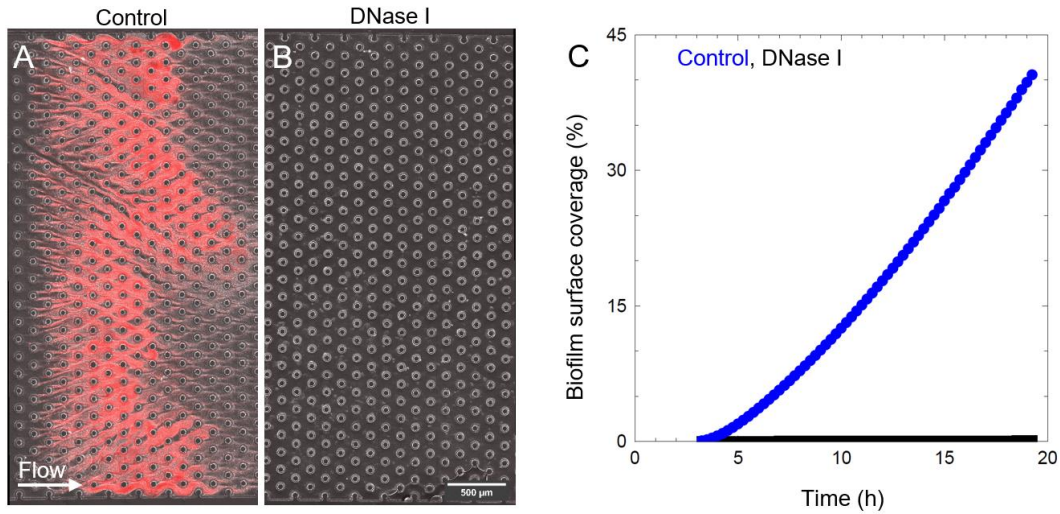
Fig. S10. DNase I prevents porous medium clogging by PA14 *WT*. (*A-B*) Overlaid phase-contrast and fluorescence representative images of the biofilm formed by *P. aeruginosa* PA14 *WT* in a model porous medium containing 75-μm pillars, after 23 h of continuous flow of a diluted bacterial suspension (*A*) and of the same suspension containing 1 mg/mL DNase I (*B*), at $U = 2$ mm/s. A portion of the porous medium is shown in the images. (*C*) Biofilm surface coverage, defined as the percentage of the image covered by the biofilm, as a function of time, measured in the same conditions as *A* (blue circles) and *B* (black squares). Biofilm coverage was measured from the fluorescence image and confirmed by comparison with the phase-contrast image.


Fig. S11. DNase I treatment reduces clogging of porous media by established PA14 *WT* biofilms. Representative phase-contrast (top) and red-fluorescence (PI, 2 μg/mL; bottom) images of the biofilm formed by *P. aeruginosa* PA14 *WT* in a model porous medium after 20 h (*A, C*) of continuous flow of a dilute bacterial suspension at $U = 2$ mm/s, and after 1.5 h flow of 1 mg/mL DNase I in PBS (*B, D*). Two positions in the channel are selected, one in the region clogged by biofilms (*A, B*) and one in the region where just biofilm streamers are present (*C, D*). The treatment depletes the eDNA in the clogged region, as can be seen from the abrupt reduction of the PI signal, and completely clears the region colonized by biofilm streamers.
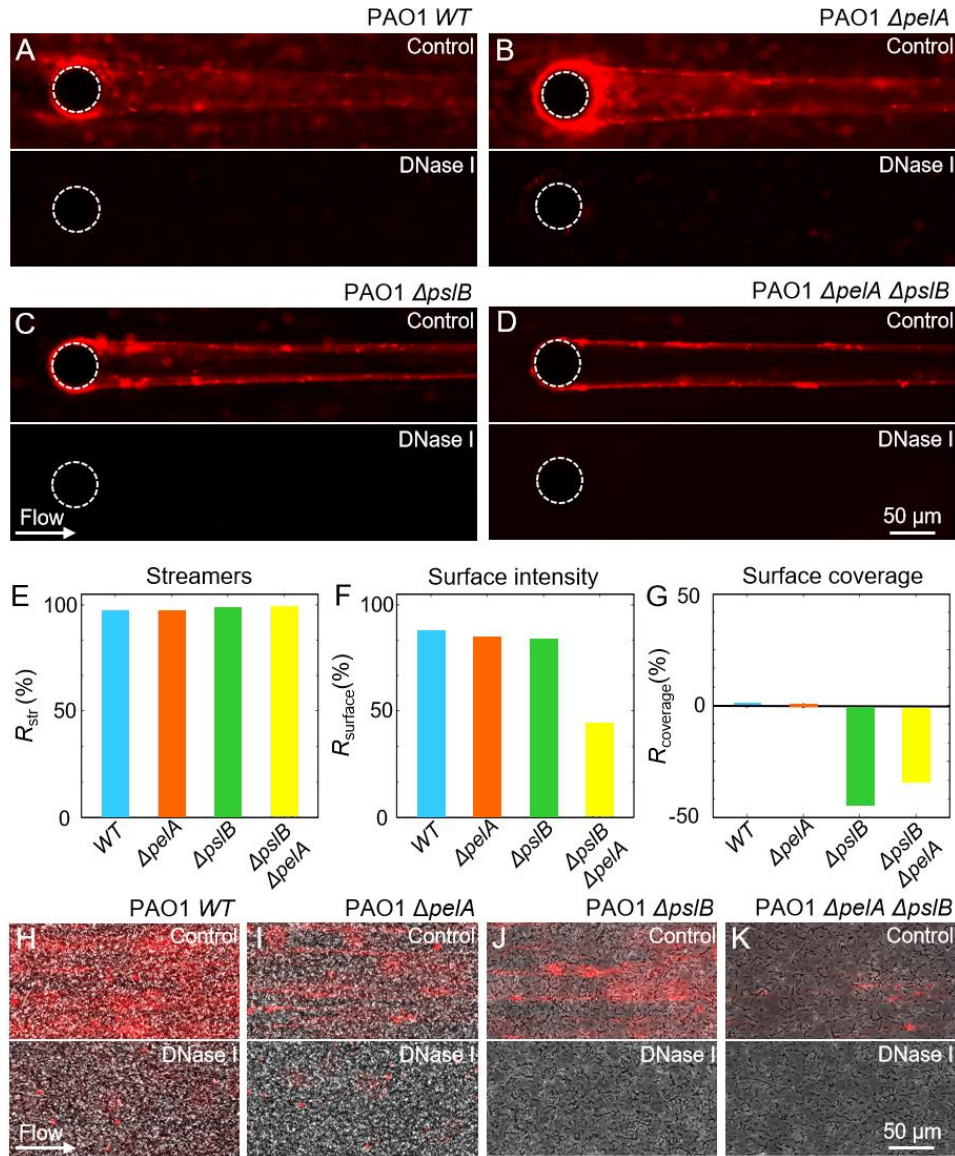
Figure S12. DNase I prevents biofilm streamer formation by PAO1. (*A–D*) Representative fluorescence images (eDNA stained using red-fluorescent PI) of biofilm streamers formed by *P. aeruginosa* PAO1 *WT (A),* PAO1 *ΔpelA (B),* PAO1 *ΔpslB* (*C*) and PAO1 *ΔpelA ΔpslB (D)* cells attached to a 50-µm pillar after 24 h of continuous flow of a dilute bacterial suspension at U = 2 mm/s, untreated (*upper panels*) or treated (*lower panels*) with 1 mg/mL DNase I. (*E–G*) Reduction after 24 h of DNase I treatment in comparison to a control channel with no DNase treatment, for R_{str}, the fluorescence intensity of the streamers (*E*), $R_{surface}$, the fluorescence intensity of the eDNA on the lower surface of the microfluidic channel (*F*), and $R_{coverage}$, the bacterial surface coverage (*G*), shown for *P. aeruginosa* PAO1 *WT* (light blue), *ΔpelA* (orange), *ΔpslB* (green), and *ΔpelA ΔpslB* (yellow). (*H–K*) Overlaid phase-contrast (bacteria) and fluorescence (eDNA) images of the biofilm formed on the lower surface by PAO1 *WT (H),* PAO1 *ΔpelA (I),* PAO1 *ΔpslB* (J) and PAO1 *ΔpelA ΔpslB (K)* cells after 18 h of continuous flow of a diluted bacterial suspension at U = 2 mm/s, untreated (*upper panels*) or treated (*lower panels*) with 1 mg/mL DNase I.
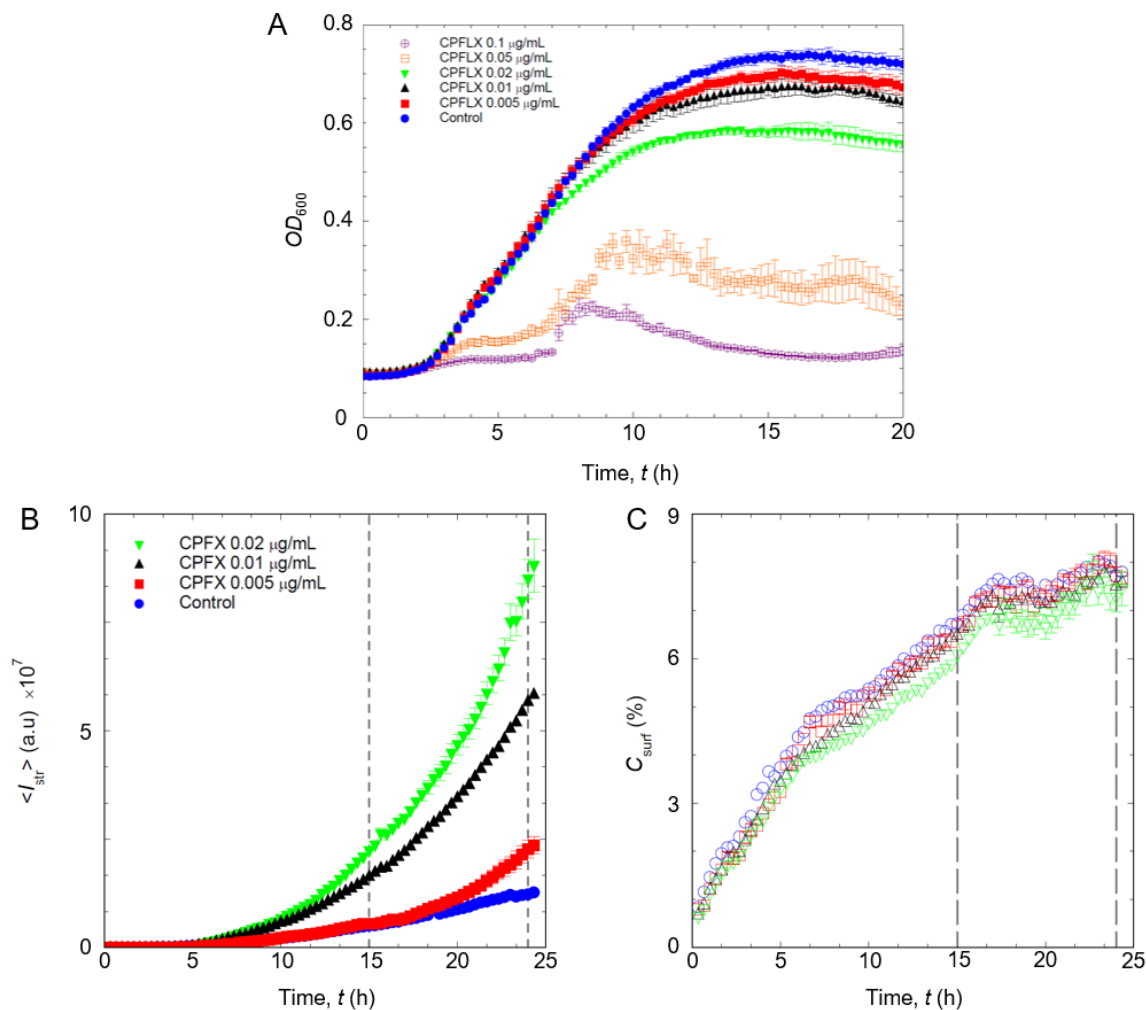
Fig. S13. Effect of ciprofloxacin at different concentrations on PA14 *WT* growth. (*A*) Population growth (*OD*$_{600}$) of *P. aeruginosa* PA14 *WT* in suspension at 37 °C in Tryptone Broth containing different concentrations of ciprofloxacin. Blue circles represent the untreated control. Each curve represents the average of six biological replicates. Error bars indicate the standard deviation from the mean. (*B*) Fluorescence intensity of streamers, $\langle \bar{I}_{str} \rangle$, formed by a dilute suspension of *P. aeruginosa* PA14 *WT* in flow at $U = 2$ mm/s as a function of time, for different concentrations of ciprofloxacin (CPFLX) (blue, no ciprofloxacin; red, 0.005 μg/mL; black, 0.01 μg/mL; green, 0.02 μg/mL). (*C*) Surface coverage (percentage), C_{surf}, as a function of time, measured on the glass surface 3 mm upstream from the pillar in the phase-contrast images under the same conditions as *B*. Dashed gray lines indicate the time points at which the intensity and surface coverage reported in Fig. 5 *E* and *J* were measured.
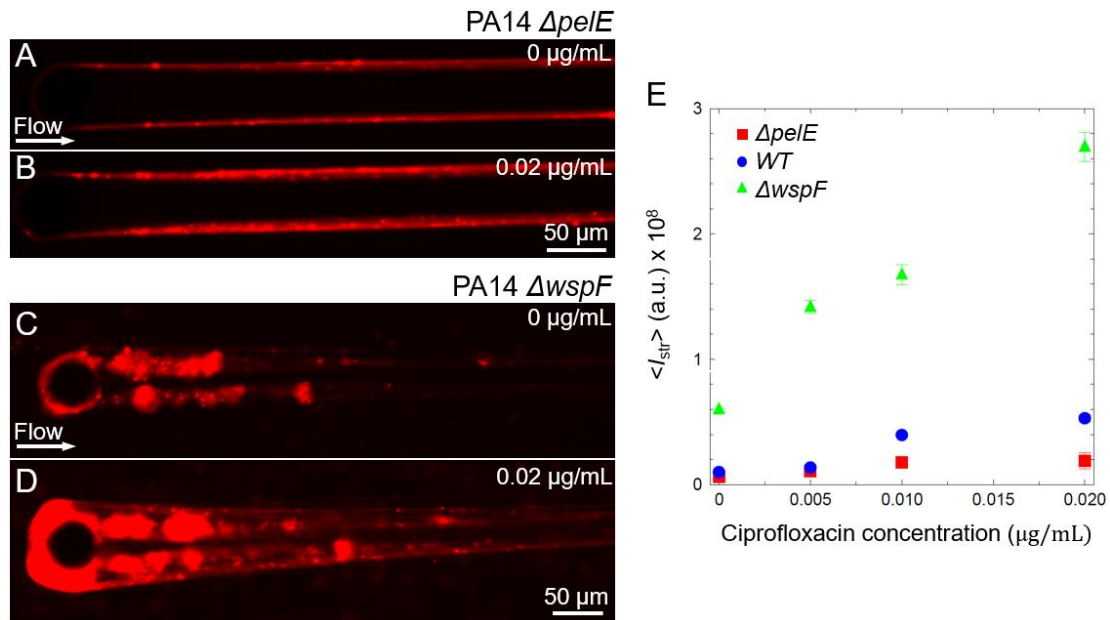
Fig. S14. Ciprofloxacin increases streamer growth for both the Pel-deficient strain PA14 *ΔpelE* and Pel-overproducer strain *ΔwspF*. (*A-D*) Representative fluorescence images of the biofilm streamers formed by *P. aeruginosa* PA14 *ΔpelE* (*A-B*) and *ΔwspF* (*C-D*) attached to a 50-µm pillar after 21 h of continuous flow at $U = 2$ mm/s of a dilute bacterial suspension containing no ciprofloxacin (*A, C*) and ciprofloxacin at a concentration of 0.02 µg/mL (*C, D*). (*E*) Fluorescence intensity of the streamers measured after 21 h of continuous flow at $U = 2$ mm/s, $\langle \bar{I}_{\mathrm{str}} \rangle$, as a function of ciprofloxacin concentration for a suspension of PA14 *WT* (blue circles), PA14 *ΔpelE* (red squares) and PA14 *ΔwspF* (green triangles). The error bar is calculated as the standard error of the mean.
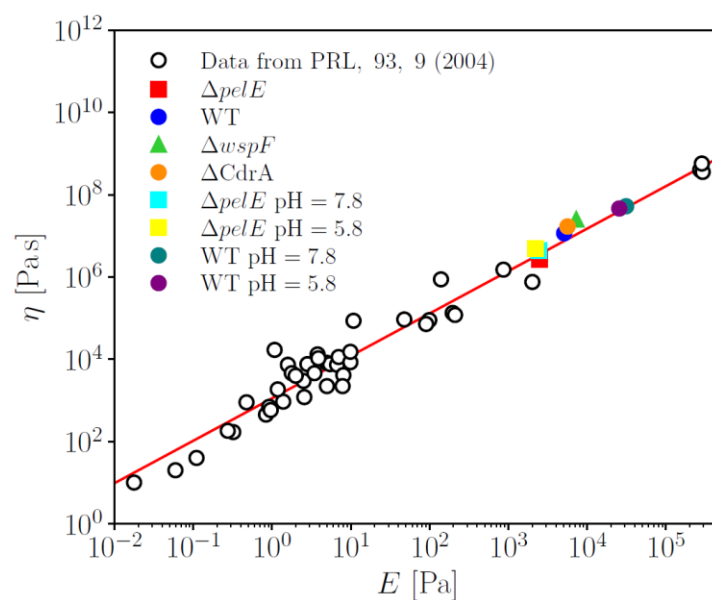
Fig. S15. Universal scaling of the elastic relaxation time η / E. Plot of young modulus E vs effective viscosity η for data taken from Fig. 3 of (10) (black circles) and for data measured in this work for PA14 *WT* (blue circles at pH 6.6, green circles at pH 7.8, purple circle at pH 5.8), PA14 *ΔpelE* (red squares at pH 6.6, yellow squares at pH 5.8 and light blue squares at pH 7.8), PA14 *ΔwspF* (green triangles), and PA14 *ΔCdrA* (orange circles). The straight red line is $\log \eta = 1.03 \, \log E + 1100$, also reported in (10). Our data follow the scaling found in (10).
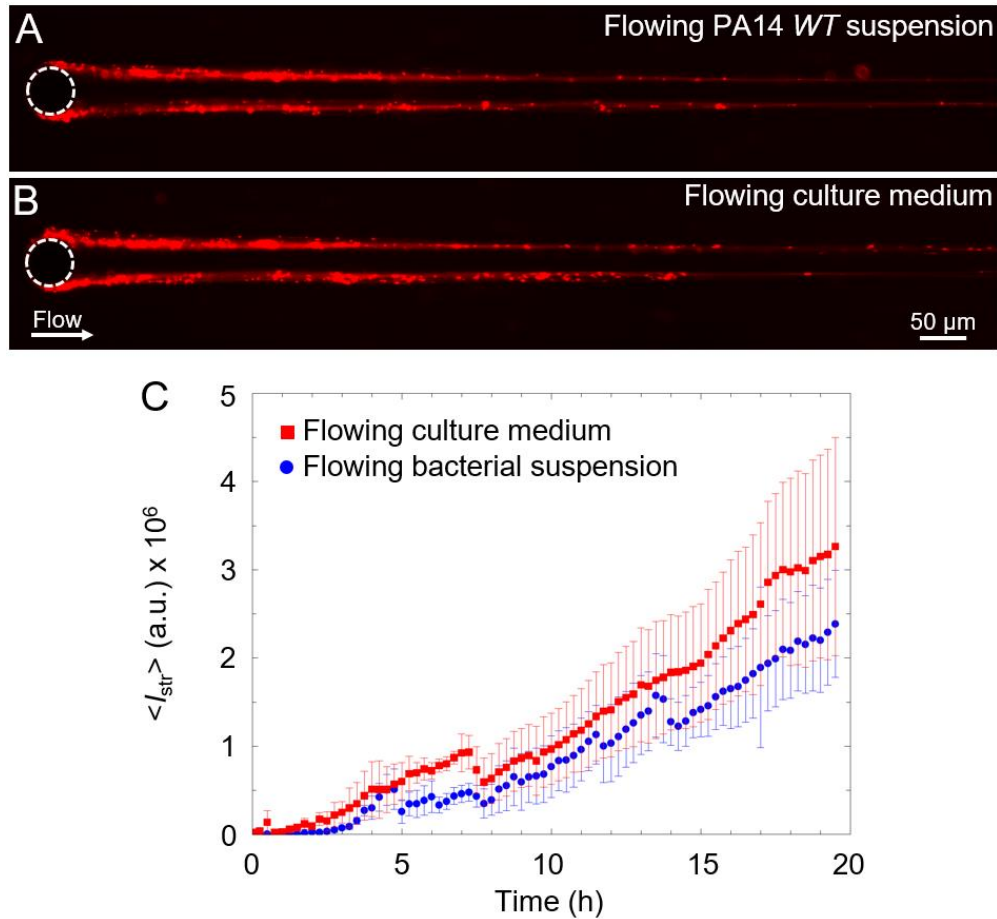
Fig. S16. Two different cell-seeding protocols do not affect streamer formation. (*A,B*) Red fluorescence (PI staining) representative images of biofilm streamers formed by flowing a dilute suspension of *P. aeruginosa* PA14 *WT* (*A*) and by flowing pure culture medium after seeding PA14 *WT* cells in the microfluidic channel (*B*). In both cases, streamers are formed on a 50-μm pillar after 20 h of continuous flow at U = 2 mm/s. In (*A*), the bacterial suspension was prepared according to the procedure presented in the manuscript. In (*B*), the microfluidic channel was filled with a PA14 *WT* bacterial suspension at OD_{600} = 0.1 and cells were left to attach for 1 h before the flow of fresh culture medium was started. (*C*) Red fluorescence intensity of streamers, $\langle \bar{I}_{str} \rangle$, corresponding to the eDNA content, as a function of time, for streamer growth when a dilute bacterial suspension was flown as in (*A*) (blue circles), and when pure culture medium was flown in the channel after prior bacterial colonization as in (*B*) (red squares). Curves were obtained by averaging the fluorescent signal measured on four different pillars. Error bars represent the standard error of the mean.

Movie S1 (separate file). DNase I prevents porous medium clogging by PA14 *WT*. Red-fluorescence image (PI, 2 µg/mL) of the biofilm formed by *P. aeruginosa* PA14 *WT* in the model porous medium during 20 h of continuous flow of a diluted bacterial suspension (left) and of the same suspension containing 1 mg/mL DNase I (right), at $U = 2$ mm/s.

Movie S2 (separate file). DNase I treatment reduces porous medium clogging by PA14 *WT*. Phase contrast (top) and red-fluorescent (PI, 2 µg/mL; bottom) image of the biofilm formed by *P. aeruginosa* PA14 *WT* in the model porous medium during 20 h of continuous flow of a diluted bacterial suspension at $U = 2$ mm/s and then washed for 3 hours with a 1 mg/mL DNase I solution. In the movie, the 3 h DNase I treatment is shown. Two positions in the channel are selected, one in the region clogged by biofilms (left) and one in the region where just biofilm streamers (right) are present.

SI References

1.   J. Schindelin, *et al.*, Fiji: An open-source platform for biological-image analysis. *Nat. Methods* **9**, 676–682 (2012).
2.   C. Haber, D. Wirtz, Shear-induced assembly of λ-phage DNA. *Biophys. J.* **79**, 1530–1536 (2000).
3.   M. S. Yeom, J. Lee, The mechanism of the self-assembly of associating DNA molecules under shear flow: Brownian dynamics simulation. *J. Chem. Phys.* **122**, 184905 (2005).
4.   C. Hsieh, A. Balducci, P. S. Doyle, An experimental study of DNA rotational relaxation time in nanoslits. 5196–5205 (2007).
5.   L. Turnbull, *et al.*, Explosive cell lysis as a mechanism for the biogenesis of bacterial membrane vesicles and biofilms. *Nat. Commun.* **7**, 11220 (2016).
6.   M. Allesen-holm, *et al.*, A characterization of DNA release in *Pseudomonas aeruginosa* cultures and biofilms. *Mol. Microbiol.* **59**, 1114–1128 (2006).
7.   C. K. Stover, *et al.*, Complete genome sequence of *Pseudomonas aeruginosa* PAO1 , an opportunistic pathogen. *Nature* **406**, 959 (2000).
8.   L. K. Jennings, *et al.*, Pel is a cationic exopolysaccharide that cross-links extracellular DNA in the *Pseudomonas aeruginosa* biofilm matrix. *Proc. Natl. Acad. Sci.* **112**, 11353–11358 (2015).
9.   C. Reichhardt, *et al.*, The versatile *Pseudomonas aeruginosa* biofilm matrix protein CdrA promotes aggregation through different extracellular exopolysaccharide interactions. *J. Bacteriol.* **202**, 1–9 (2020).
10.   T. Shaw, M. Winston, C. J. Rupp, I. Klapper, P. Stoodley, Commonality of elastic relaxation times in biofilms. *Phys. Rev. Lett.* **93**, 098102 (2004).